PERGAMON

Atmospheric Environment 34 (2000) 3015–3026

ATMOSPHERIC ENVIRONMENT

www.elsevier.com/locate/atmosenv

Comparison of a 4000-reaction chemical mechanism with the carbon bond IV and an adjusted carbon bond IV-EX mechanism using SMVGEAR II

Jinyou Liang, Mark Z. Jacobson*

Department of Civil and Environmental Engineering, Stanford University, Stanford, CA 94305-4020, USA

Received 17 August 1999; accepted 22 October 1999

Abstract

The well-known carbon bond IV (CBIV) chemical mechanism (33 species, 81 reactions) is compared with an adjusted carbon bond mechanism (ACBM) (109 species, 233 reactions) and a more explicit master chemical mechanism (MCM) (1427 species, 3911 reactions) in tests of their predictions of O_3, $NO_x(=NO+NO_2)$, HCHO, HNO_3, H_2O_2, and peroxyacetlynitrate (PAN). The ACBM was developed from a fourth mechanism, the expanded carbon bond mechanism (CBM-EX), by explicitly including the decomposition of C_2H_6, C_3H_8, and C_3H_6. All three mechanisms tested were updated with the inorganic chemistry from the ACBM and implemented into the sparse-matrix, ordinary differential equation solver, SMVGEAR II. Sparse-matrix treatment in SMVGEAR II reduced the number of calculations during matrix decomposition for the MCM by a factor of 15,000 (99.995%), or from an estimated 154 h to 37 s of cpu time per simulation day in one grid cell on an SGI origin 2000, in comparison with a full-matrix solution. Computer time for each mechanism was linearly proportional to the number of species in the mechanism. It is shown that the three mechanisms agreed closely when aromatic concentrations were initially low in comparison with alkane, alkene, and aldehyde initial concentrations. When aromatic concentrations were initially high (higher than that observed in urban air), the yields of O_3, HCHO, and PAN differed significantly among the three mechanisms although the daily maximum concentrations of these species agreed better. The aromatic representation in MCM appears to lead to systematic overprediction of ozone, according to a comparison with smog chamber data. For initial conditions taken from measurements at nine sites in Los Angeles, the daily maximum concentrations of O_3, HCHO, PAN, and H_2O_2 predicted by the three mechanisms differed by 30–50%, 10–40%, 15–40%, and 60–80%, respectively. The relative differences between the daytime series of O_3, HCHO, H_2O_2, and PAN predicted by the three mechanisms were 7–68%, 7–46%, 35–150%, and 10–64%, respectively. The use of the aromatic scheme of ACBM in MCM significantly reduced the disagreement with respect to ozone. The measurement of H_2O_2 in smog chamber experiments would be useful in validating chemical mechanisms. © 2000 Elsevier Science Ltd. All rights reserved.

1. Introduction

Considerable effort has been devoted to understanding oxidant formation on urban, regional and global scales. As a result, a number of photochemical reaction mechanisms are now available for air quality modeling (Whitten et al., 1980; Atkinson et al., 1982; Stockwell, 1986; Lurmann et al., 1987; Gery et al., 1989; Carter, 1990; Madronich and Calvert 1990; Stockwell et al., 1990, 1997). An outstanding issue facing photochemical modelers is the balance between computing efficiency, which favors compressed chemical mechanisms and accuracy, which demands explicit treatment of chemical reactions and, therefore, favors large chemical mechanisms.

* Corresponding author. Tel.: +1-650-723-6836; fax: +1-650-725-9720.

E-mail address: jacobson@ce.stanford.edu (M.Z. Jacobson).

1352-2310/00/$ - see front matter © 2000 Elsevier Science Ltd. All rights reserved.
PII: S1352-2310(99)00486-0

Here, we compare three chemical mechanisms of varying degrees of explicit treatment. Two of the mechanisms have been used in three-dimensional air quality models, whereas, the most explicit mechanism has not. The first mechanism is the carbon bond IV (CBIV) mechanism (Gery et al., 1989), which contains 33 species or lumped carbon-bond groups and 81 reactions. Among the lumped groups are PAR (single carbon atoms), OLE (terminal carbon atom pairs with a double bond between the two atmos), ALD2 (non-terminal carbon atom pairs with a double bond attached to one of the carbons and terminal two-carbon carbonyl groups), TOL (monoalkylbenzenes), and XYL (dialkyl and trialkylbenzenes). We modified the inorganic portion of the original CBIV mechanism, as described shortly. Thus, the number of reactions in the CBIV mechanism was increased to 93, including 41 inorganic kinetic reactions (the first 41 reactions of ACBM as described below), 40 organic kinetic reactions, and 12 photolysis reactions. The original CBIV mechanism has been used in a variety of studies (Chock et al., 1995; Hertel et al., 1995; Kasibhatla et al., 1997; Houweling et al., 1998). We note that the addition of HO_2–RO_2 reactions (Kasibhatla et al., 1997) to the original CBIV would probably improve the prediction of H_2O_2 from this mechanism, but we do not include those reactions in the original CBIV in this study.

The second mechanism compared is referred to here as the adjusted carbon bond mechanism (ACBM) and consists of 109 species and 233 reactions (41 kinetic inorganic, 167 kinetic organic, and 25 photolysis). The reactions are listed in p. 591–600 in Table B.4 of Jacobson (1999a) (see also http://efml.stanford.edu/FAMbook/FAMbook.html for corrections to the mechanism as printed). The reactions included are 1, 5–6 (combined into one), 10–48, 51–217, 298–299, 301–304, 306–316, 320–326, and the photolysis of CH_3ONO. The mechanism was derived from the expanded carbon bond IV mechanism of Gery et al. (1989) by replacing the inorganic portion with updated reactions and rate coefficients from Atkinson et al. (1997) and DeMore et al. (1997), adding explicit treatment of ethane (C_2H_6), propane (C_3H_8), and propene (C_3H_6) from data in Atkinson et al. (1997) and updating other explicit organic rate coefficients where possible. The hemiterpene portion of the mechanism was also updated, but terpene and hemiterpene chemistry is not discussed here, since the most explicit mechanism, discussed next, does not include it. Various versions of the ACBM have been applied to air quality studies in Los Angeles (Jacobson et al., 1996; Jacobson, 1997, 1998a, 1999b,c).

The third mechanism discussed is referred to as the Master Chemical Mechanism (MCM). It contains 1427 species and 3911 reactions (41 kinetic inorganic, 2956 kinetic organic, and 914 photolysis) and was extracted from a larger list of reactions complied by Jenkin et al. (1997) (http://chem.leeds.ac.uk/Atmospheric/MCM/main.html#Master). The species selected were chosen because they were on a list of or were derivatives of about 35 organic gases, identified in Table 12.4 of Jacobson (1999a), that are emitted in the Los Angeles Basin in the greatest quantity. Hence, the MCM used here includes reactions for organics that are byproducts of major emitted species but neglects additional reactions available from Jenkin et al. (1997) for organics that are byproducts of lesser important species. For consistency, the inorganic portions of all three mechanisms were taken from the inorganic portion of the ACBM (reactions listed in p. 591–592 in Table B.4. of Jacobson (1999a). The MCM describes the complete tropospheric oxidation of alkenes up to nonane, of alkenes up to pentene, of aldehydes up to pentanol, of ketones up to hexanone, and of aromatics up to trimethylbenzene. It does not include the formation of cresol and aromatic nitrates. A complete list of species and reactions is available upon request from jacobson@ce.stanford.edu.

All three mechanisms were implemented into the sparse-matrix, ordinary differential equation solver, SMVGEAR II (Jacobson and Turco, 1994; Jacobson, 1995,1998b) and simulations were run to compare results from the three mechanisms. This scheme was chosen partly because it used Gear's solution mechanism, which is considered to be accurate, but also because the scheme minimizes computer time and array space by applying sparse-matrix techniques during matrix decomposition and backsubstitution. Without both computer time and array-space reductions, simulation with the MCM mechanism, even in one grid cell, would be challenging. Simulations in a three-dimensional model would not be possible with current computer resources. A final reason to use SMVGEAR II is that the scheme allows the input of any number of reactions without the need to modify the code, except for changing dimensions. This feature is important with a mechanism of 4000 reactions.

Two types of simulations were carried out. In the first, concentrations were initialized with the same concentrations used in several smog-chamber experiments. In the second, concentrations were initialized with data, measured during the Southern California Air Quality Study (SCAQS), from nine sites in the Los Angeles basin.

Our study differs from previous mechanism comparisons (e.g. Dodge, 1989; Andersson-Skold and Simpson, 1999) in that (1) we compare three mechanisms of various explicit organic treatment rather than mechanisms of similar size but different lumping assumptions, and (2) we compare two mechanisms not previously compared with smog chamber data or other mechanisms.

2. Comparisons under smog-chamber conditions

For our first comparison, we compiled a series of initial mixing ratios from smog-chamber experiments (Jeffries

Table 1
Initial mixing ratios[a]

Case	Species	CBIV	ACBM	MCM
(a) HCHO case				
	HCHO	1000	1000	1000
	NO	500	500	500
	NO_2	500	500	500
(b) C_2H_4 case				
	PAR	20	20	
	i-C_4H_{10}			2.5
	n-C_4H_{10}			2.5
	C_2H_4	500	500	500
	OLE	0.3	0.3	
	C_3H_6			0.2
	Toluene	0.06	0.06	0.06
	m-Xylene	0.036	0.036	0.036
	HCHO	3.8	3.8	3.8
	CH_3CHO	1.5	1.5	1.5
	NO	100	100	100
	NO_2	100	100	100
(c) C_3H_6 case				
	PAR	220	20	
	i-C_4H_{10}			2.5
	n-C_4H_{10}			2.5
	C_2H_4	0.45	0.45	0.45
	OLE	200	0	
	C_3H_6		200	200
	Toluene	0.06	0.06	0.06
	m-Xylene	0.036	0.036	0.036
	HCHO	3.8	3.8	3.8
	CH_3CHO	1.5	1.5	1.5
	NO	100	100	100
	NO_2	100	100	100
(d) Toluene-UNC62784 case				
	C_2H_4	122	122	122
	Toluene	702	702	702
	NO	300	300	300
	NO_2	35	35	35
	HONO	2.45	2.45	2.45
(e) Xylene-UNC62784 case				
	C_2H_4	130	130	130
	m-Xylene	249	249	249
	NO	303	303	303
	NO_2	41	41	41
	HONO	2.87	2.87	2.87

[a]Note: Units are ppbv. The initial mixing ratios of CO, O_3, and water vapor were 310 ppbv, 30 ppbv, and 1%, respectively, in cases a–c, and were 300 ppbv, 0 ppbv, and 2% in case d–e. The unlisted reactive species were initialized with a negligible mixing ratio. PAR and OLE are lumped species as in the carbon bond mechanism (Gery et al., 1989). Temperature is 298 K, and the altitude is 0 km.

et al., 1988). The initial conditions are given in Table 1 and were categorized as 'HCHO', 'C_2H_4', 'C_3H_6', 'toluene', and 'xylene' cases. Each case-name was defined based on the species with the highest mixing ratio in the case.

The time-series mixing ratios of NO, NO_2, NO_3, HNO_3, H_2O_2, and HCHO in the HCHO case agree within 5% (not shown), which results from the use of virtually the same inorganic chemistry and HCHO decomposition scheme in all three mechanisms. In the C_2H_4 and C_3H_6 cases, the agreement is within 20% for all compared species (not shown), except H_2O_2, even though these cases involve composite initial conditions. For H_2O_2, the disagreement between the three mechanisms ranges from 20–70%. The inclusion of the explicit decomposition mechanism of C_3H_6 in the ACBM contributes to the good agreement with the MCM.

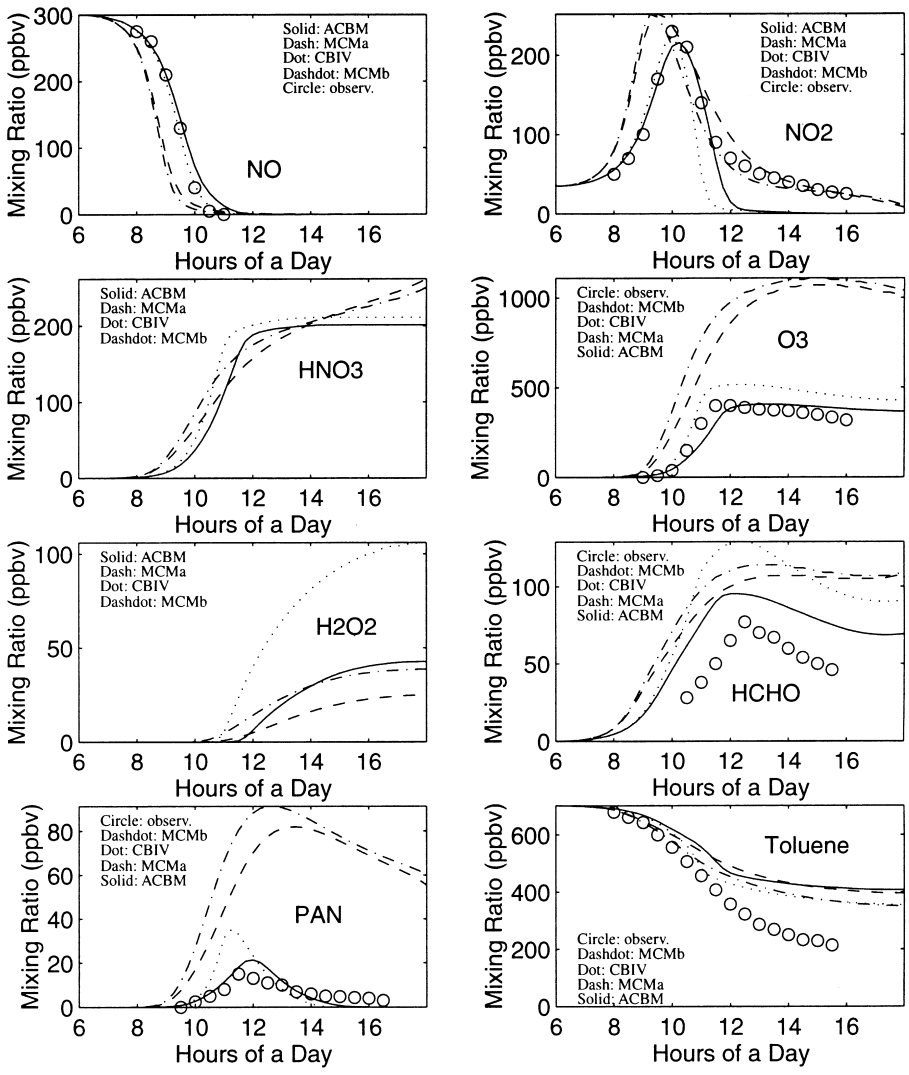

Fig. 1. Time series of NO, NO_2, O_3, HNO_3, H_2O_2 and HCHO in the toluene case using CBM-IV, ACBM, and MCM mechanisms, respectively.

We compiled initial conditions (Table 1 d and e) pertinent to the University of North Carolina outdoor smog chamber experiments for the decomposition of toluene and *m*-xylene conducted on 27 June 1984. We use photolysis rates from Gery et al. (1988) and the Carter's wall reaction rates from Jeffries et al. (1988) in all simulations. For the MCM mechanism, we conducted two simulations, including one (MCMa) with all photolysis reactions, other than those listed in CBIV, turned off, and the other (MCMb) with all photolysis reactions, other than those listed in CBIV, set to an estimated maximum photolysis rates (Jenkin et al., 1997). The results for the toluene and xylene cases are shown in Figs. 1 and 2, respectively. Compared with the observed time series of NO, NO_2, O_3, HCHO, and PAN for the outdoor smog chamber experiments conducted at University of North Carolina on 27 June 1984, as presented by Gery et al. (1988) and Jeffries et al. (1988), the time series from ACBM appeared most consistent with observations with respect to O_3 and PAN in both cases. Additional comparisons with smog chamber studies are needed to determine whether this pattern holds up under other conditions. The absence of the formation of cresol and aromatic nitrates may partly account for the overprediction of O_3 and PAN by MCM.

3. Comparisons under SCAQS ambient conditions

For our second comparison, we compiled measurements at nine sites in the Los Angeles Basin at 6 AM

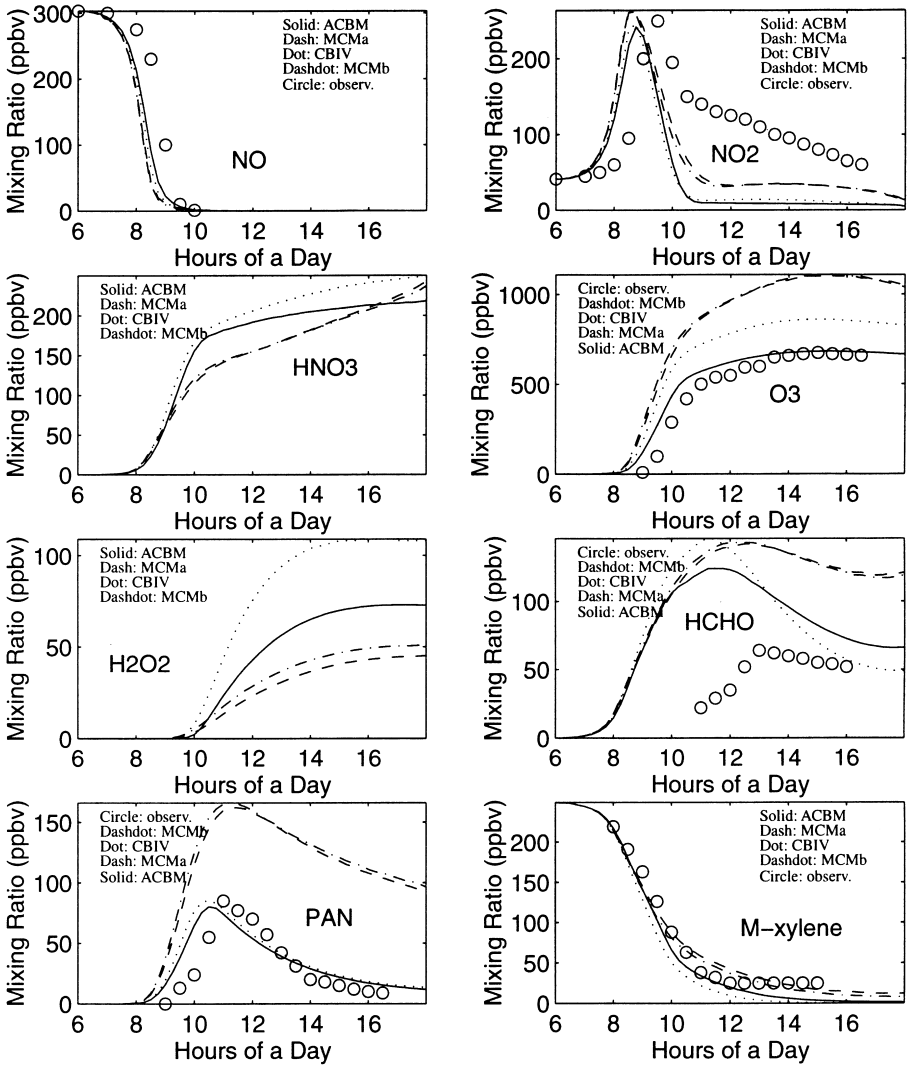

Fig. 2. Same as Fig. 1, except in the xylene case.

during 27–29 August 1987. Tables 2 and 3 list the average mixing ratios at each site for CBIV (Table 2), ACBM (Table 2), and MCM (Table 3). The partitioning of explicit-species concentrations from the MCM to carbon-bond lumping groups in CBIV and ACBM were carried out with partitioning fractions provided by the California Air Resources Board.

We ran simulations from 6 AM to 6 PM at each site using the three mechanisms. Fig. 3 shows time-series comparisons of NO_x, O_3, HNO_3, HCHO, PAN, and H_2O_2 at one site. It is shown that the MCM consumes NO_x slower but produces more O_3, compared with CBIV and ACBM. The agreement between CBIV and ACBM is close in terms of the daily maximum O_3 concentration, but CBIV and ACBM differ by 50% for the daily maximum concentration of H_2O_2. For the daily maximum concentrations of HCHO and PAN, CBIV and ACBM agree within 30%. The daily maximum concentrations of O_3, HCHO, PAN, and H_2O_2 predicted by the MCM differ from those predicted by CBIV and ACBM by up to 50, 40, 40, and 80%, respectively, at all nine sites.

Table 4 lists the mean mixing ratios for a list of species in the three mechanisms from 6 AM to 6 PM and the time-averaged differences among the mechanisms at nine sites. The equation used for determining the time-averaged difference (TAD) is

$$\mathrm{TAD} = \frac{1}{n}\sum_{t=1}^{n} |C_t - C_t'|, \tag{1}$$

where n is the number of points in the time series, and C_t and C_t' denote the mixing ratios of the two time series

Table 2
Initial mixing ratios for the CBIV and ACBM mechanisms at nine sites[a]

Species	ANAH	AZUS	BURK	CELA	CLAR	HAWT	LBCC	RIVR	SNI
(a) CBIV									
CO	1575.3	1896.5	3561.5	2839.0	2871.7	809.3	1516.0	2595.0	154.5
OLE	8.0	14.2	35.2	19.3	16.3	11.9	21.2	27.6	0.8
PAR	1527.3	1719.2	2975.1	2025.2	2046.0	841.6	1949.2	2165.8	146.6
TOL	58.9	96.3	149.1	108.4	110.0	30.1	56.0	97.8	4.4
XYL	68.8	108.5	159.9	123.3	120.8	32.6	62.6	114.2	7.6
HCHO	12.8	6.7	12.5	8.8	11.1	10.3	10.6	14.9	4.3
ALD2	37.0	25.5	49.9	30.5	37.5	17.4	38.3	63.6	19.3
C_2H_4	16.2	15.1	52.8	19.1	39.9	14.9	30.6	33.4	0.7
NO	110.0	30.0	160.0	90.0	43.0	20.0	82.0	120.0	3.1
NO_2	60.0	50.0	50.0	50.0	57.0	30.0	46.0	20.0	3.1
O_3	10.0	10.0	10.0	0.0	3.0	10.0	5.0	0.0	30.0
(b) ACBM									
CO	1575.3	1896.5	3561.5	2839.0	2871.7	809.3	1516.0	2595.0	154.5
CH_4	2306.0	2391.0	2654.0	2341.0	2268.0	1949.0	2171.3	3323.5	1710.0
C_2H_6	20.3	12.9	88.4	26.0	35.4	19.4	45.6	37.2	0.9
C_3H_8	45.4	47.6	169.4	60.8	56.2	39.0	92.6	60.2	1.8
C_3H_6	5.4	10.1	27.4	15.5	13.4	9.0	16.3	23.3	0.5
OLE	2.6	4.0	7.9	3.8	2.9	2.9	4.9	4.3	0.2
PAR	1422.6	1608.6	2631.8	1884.7	1911.4	746.8	1754.1	2004.1	125.9
TOL	58.9	96.3	149.1	108.4	110.0	30.1	56.0	97.8	4.4
XYL	68.8	108.5	159.9	123.3	120.8	32.6	62.6	114.2	7.6
HCHO	12.8	6.7	12.5	8.8	11.1	10.3	10.6	14.9	4.3
CH_3CHO	37.0	25.5	49.9	30.5	37.5	17.4	38.3	63.6	19.3
C_2H_4	16.2	15.1	52.8	19.1	39.9	14.9	30.6	33.4	0.7
KET	4.9	15.8	12.0	10.4	8.8	1.3	6.4	23.2	2.0
NO	110.0	30.0	160.0	90.0	43.0	20.0	82.0	120.0	3.1
NO_2	60.0	50.0	50.0	50.0	57.0	30.0	46.0	20.0	3.1
O_3	10.0	10.0	10.0	0.0	3.0	10.0	5.0	0.0	30.0

[a]Note: Units are ppbv. The initial mixing ratios are the averages from measurements at 6 AM on 27, 28 and 29 August 1987. OLE, PAR, ALD2, KET, TOL, and XYL are lumped species from the carbon bond mechanism (Gery et al., 1989). The temperature and pressure were assumed to be 298 K and 1013 mb, respectively, NO, NO_2, and O_3 at SNI were assumed due to the lack of measured values.

in comparison at time t. The time-averaged difference ranges from 5 to 230 ppbv for O_3, 1–16 ppbv for HCHO, 2–50 ppbv for H_2O_2, and 0.5–18 ppbv for PAN, as shown in Table 4. Let us define the relative difference (RD) as the time-averaged difference divided by the mean mixing ratio of the three time series,

$$\mathrm{RD} = \frac{\mathrm{TAD}}{1/3n\sum_{t=1}^{n}(C_t + C_t' + C_t'')}, \quad (2)$$

where C, C' and C'' denote the mixing ratios of the three time series of CBIV, ACBM, and MCM, respectively, and other notations are the same as in Eq. (1). The relative difference ranges from 7 to 68% for O_3, 7–46% for HCHO, 35–150% for H_2O_2, and 10–64% for PAN. At 273 K (in contrast with at 298 K, the temperature of all other comparisons), the mean mixing ratios of O_3, HCHO, H_2O_2, and HNO_3 were reduced in all mechanisms as a result of slower photochemical reactions. The mean mixing ratio of PAN increased by 50% at 273 K in comparison with at 298 K due to the slower decomposition of PAN at lower temperatures. The ratio of NO to NO_2 increased at 273 K in comparison with at 298 K, since fewer peroxy radicals were produced in the chemical system to convert NO to NO_2 at 273 K. The effect of temperature on the relative differences in the time series of O_3, HCHO, H_2O_2, and PAN was small, reflecting the same trend of the mean mixing ratios and average differences, as shown in Table 4 in an example sensitivity test at Anaheim.

We conducted additional simulations by replacing all aromatic reactions in MCM (292 reactions) with those in ACBM (26 reactions), and show the results in Fig. 3. The agreement with respect to ozone among the three

Table 3
Initial mixing ratios for the MCM at nine sites[a]

Species	ANAH	AZUS	BURK	CELA	CLAR	HAWT	LBCC	RIVR	SNI
CO	1575.3	1896.5	3561.5	2839.0	2871.7	809.3	1516.0	2595.0	154.5
CH_4	2306.0	2391.0	2654.0	2341.0	2268.0	1949.0	2171.3	3323.5	1710.0
C_2H_6	20.3	12.9	88.4	26.0	35.4	19.4	45.6	37.2	0.9
C_2H_4	16.2	15.1	52.8	19.1	39.9	14.9	30.6	33.4	0.7
C_2H_2	10.9	12.5	46.1	11.7	32.1	12.8	17.3	41.1	1.9
C_3H_8	45.4	47.6	169.4	60.8	56.2	39.0	92.6	60.2	1.8
C_3H_6	5.4	10.1	27.4	15.5	13.4	9.0	16.3	23.3	0.5
i-C_4H_{10}	23.2	17.9	34.8	20.7	21.4	15.9	30.1	20.6	0.6
n-C_4H_{10}	52.9	45.0	84.4	57.3	52.5	26.8	73.8	52.3	1.5
Trans-2-Butene	0.8	1.0	2.9	1.1	1.3	0.4	2.0	2.2	0.0
Cis-2-Butene	1.1	1.1	2.5	1.6	1.2	0.5	1.9	1.5	0.0
3-Methyl-1-Butene	0.6	0.6	1.3	1.2	0.8	0.4	0.9	0.9	0.2
i-C_5H_{12}	56.7	62.2	110.6	80.1	77.2	32.1	79.8	80.6	4.5
l-Pentene	2.0	3.3	6.6	2.7	2.1	2.5	3.9	3.4	0.0
2-Methyl-1-Butene	1.8	2.3	5.6	3.6	2.2	6.8	3.5	2.8	0.2
n-C_5H_{12}	31.6	28.5	45.5	35.2	33.8	11.9	40.8	37.5	1.6
Trans-2-Pentene	1.9	2.5	5.8	3.7	2.5	0.7	3.5	3.2	0.2
Cis-2-Pentene	1.0	1.2	3.2	2.1	1.5	0.3	2.1	1.8	0.2
2,2-Dimethylbutane	0.0	0.0	0.0	0.9	1.1	0.0	0.0	0.9	0.0
2,3-Dimethylbutane	4.6	5.7	9.9	7.2	6.8	2.5	5.8	7.5	0.3
2-Methylpentane	18.0	21.6	36.0	26.9	27.0	9.3	20.8	28.4	1.3
3-Methylpentane	12.8	14.1	25.0	17.5	17.5	6.3	14.2	18.0	1.3
n-C_6H_{14}	12.6	15.0	23.2	17.2	19.5	5.5	14.9	17.5	0.7
Benzene	18.0	22.4	40.7	30.9	30.6	9.1	19.4	30.6	1.2
Cyclohexane	3.4	3.8	6.2	5.2	4.4	1.6	4.5	4.2	0.2
2-Methylhexane	6.2	8.6	14.5	10.9	11.9	3.2	6.8	10.6	0.6
3-Methylhexane	7.6	10.2	16.5	12.7	16.0	3.9	8.2	11.9	1.0
n-C_7H_{16}	7.3	9.4	14.1	11.6	10.8	3.0	6.5	8.4	0.2
Toluene	48.7	76.5	126.4	90.2	91.6	25.5	46.5	80.9	3.8
n-C_8H_{18}	2.4	5.6	5.2	4.7	4.3	0.8	3.3	3.6	0.1
Ethylbenzene	8.4	16.5	18.5	14.6	14.6	3.8	7.7	14.0	0.6
m-Xylene	31.6	51.9	74.2	56.2	54.8	14.6	28.9	53.8	3.8
o-Xylene	11.9	18.0	26.8	19.8	19.6	6.5	10.2	19.9	2.3
n-C_9H_{20}	1.4	5.4	3.4	2.9	2.2	0.9	1.5	2.5	0.0
n-Propylbenzene	1.8	3.3	4.2	3.6	3.8	0.8	1.7	2.8	0.0
m-Ethyltoluene	7.1	10.9	16.9	13.2	13.1	3.3	6.5	11.9	0.0
p-Ethyltoluene	3.5	5.8	8.7	6.6	6.7	1.7	3.3	5.9	0.4
o-Ethyltoluene	3.3	5.7	7.7	5.8	6.5	1.5	3.1	5.1	0.0
l,2,4-Trimethylbenzene	11.6	16.2	25.7	21.8	20.0	4.9	10.6	17.7	1.0
HCHO	11.0	4.3	6.9	5.2	8.9	3.5	7.2	12.1	4.1
CH_3CHO	12.3	8.5	9.5	7.1	12.3	5.7	7.5	21.4	6.5
CH_3COCH_3	17.8	23.1	32.0	16.0	23.2	7.9	9.4	34.1	2.4
C_2H_5CHO	3.4	0.6	3.0	2.2	2.9	2.7	2.3	5.4	2.7
Methyl-ethyl-ketone	4.9	15.8	12.0	10.4	8.8	1.3	6.4	23.2	2.0
C_3H_7CHO	2.8	0.4	3.8	0.2	0.7	1.1	0.0	2.8	1.4
C_4H_9CHO	9.0	4.0	5.0	3.8	8.5	4.0	9.5	17.0	8.0
NO	110.0	30.0	160.0	90.0	43.0	20.0	82.0	120.0	3.1
NO_2	60.0	50.0	50.0	50.0	57.0	30.0	46.0	20.0	3.1
O_3	10.0	10.0	10.0	0.0	3.0	10.0	5.0	0.0	30.0

[a]Note: Units are ppbv. The initial mixing ratios are the averages from measurements at 6 AM on 27, 28, and 29 August 1987. The temperature and pressure were assumed to be 298 K and 1013 mb, respectively. NO, NO_2, and O_3 at SNI were assumed due to the lack of measured values.

mechanisms is now close, indicating that the original treatment of aromatics in MCM was responsible for the significant disagreement of ozone in Fig. 3. Since the atmospheric reactivity of many intermediate species in MCM is poorly understood, the uncertainties in the hypothetical chemical reactions of these species and the

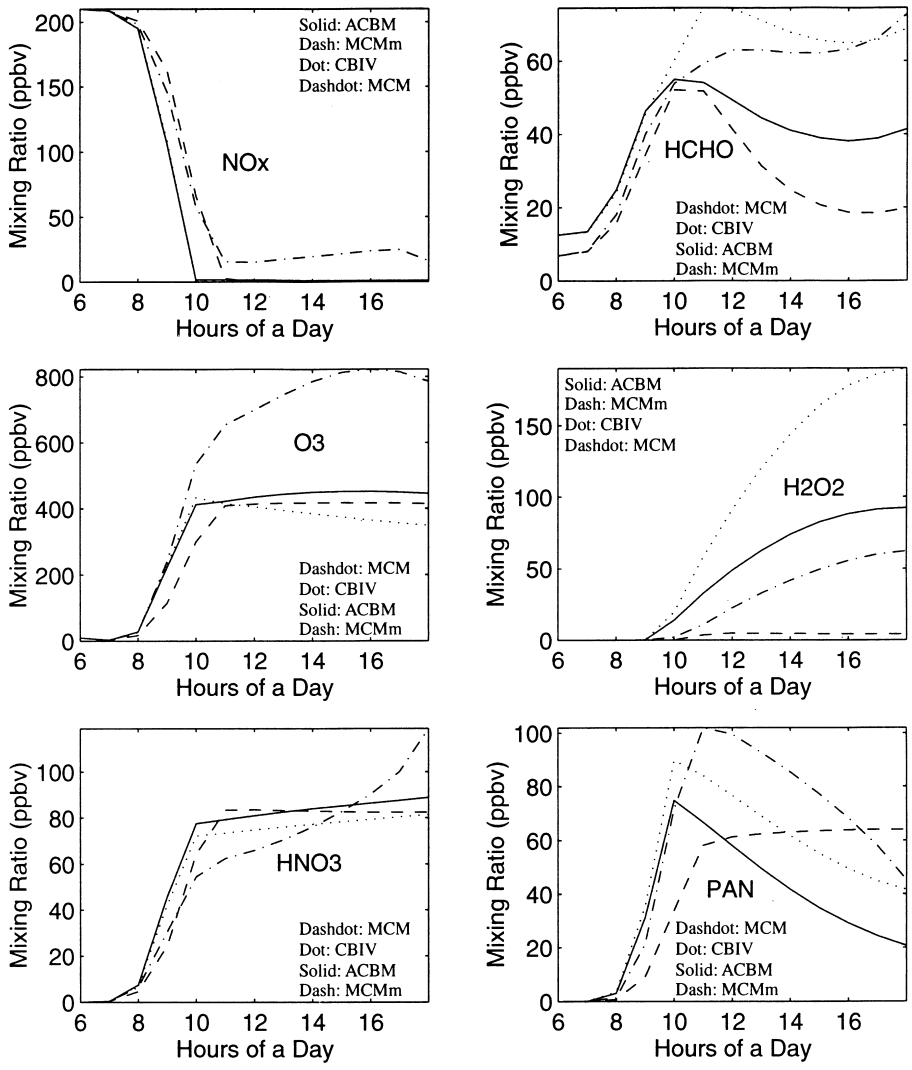

Fig. 3. Time series of NO_x, O_3, HNO_3, HCHO, PAN, and H_2O_2 using CBIV, ACBM, and MCM mechanisms, respectively, with initial conditions measured at site BURK. MCMm is same as MCM except that the aromatic scheme of MCM is now replaced by that of ACBM.

hypothetical reaction rate constants may be also responsible for the large difference in other species compared in Fig. 3. The measurement of H_2O_2 in smog chamber experiments would be useful in validating chemical mechanisms, since the disagreement among the three mechanisms is the most outstanding.

4. Computer timings and sparse-matrix reductions from SMVGEAR II

One finding of this study is that the use of sparse-matrix techniques in SMVGEAR II during MCM calculations resulted in a reduction in multiplications during matrix decomposition by a factor of 13,448 (99,995%) during the day and 16,810 (99.996%) at night in comparison with a full-matrix solution (Table 5). The savings for the MCM was more considerable than for the ACBM (99.50–99.52%) or the CBIV (94.09–94.43%). The computer time for each mechanism (Table 6) was almost linearly dependent on the number of species included in the solution matrix (the order of matrix term in Table 5), with the regression *R*-square of 0.9998 for a one-box simulation and of 0.9995 for a 500-box simulation on an SGI Origin 2000. On a Cray J90, the corresponding regression *R*-square is 0.9999 for both a one-box

Table 4
Average difference (ppbv) of the time series between the three mechanisms at nine sites[a]

Case	HCHO	NO	NO_2	O_3	H_2O_2	HNO_3	PAN
ANAH (298 K)							
Mean Value	25.30	24.39	37.91	297.2	18.94	52.35	29.28
ACBM-MCM	5.977	1.890	14.44	131.7	7.226	4.928	7.014
MCM-CBIV	1.723	1.824	14.66	144.1	22.13	5.212	3.059
ACBM-CBIV	6.254	0.0878	0.2338	19.45	14.90	2.608	8.860
ANAH (273 K)							
Mean Value	14.49	29.55	36.37	215.6	10.33	40.97	43.96
ACBM-MCM	3.831	2.020	3.742	63.49	1.844	7.875	8.903
MCM-CBIV	2.354	6.077	6.711	108.2	3.459	3.566	1.737
ACBM-CBIV	4.431	4.170	5.241	44.74	4.541	9.521	9.572
AZUS (298 K)							
Mean Value	23.70	5.140	16.79	241.8	34.14	18.57	19.35
ACBM-MCM	8.238	1.046	8.508	134.8	13.53	3.814	13.27
MCM-CBIV	3.642	1.055	8.904	159.5	44.10	2.736	8.456
ACBM-CBIV	11.00	0.0781	0.4382	27.68	30.58	1.599	5.874
BURK (298 K)							
Mean Value	47.52	27.70	34.98	389.2	53.31	57.03	46.65
ACBM-MCM	13.92	2.416	20.82	228.2	18.86	10.92	27.02
MCM-CBIV	5.278	2.524	20.92	264.9	62.26	7.637	16.12
ACBM-CBIV	16.41	0.1155	0.4997	41.29	43.43	4.840	13.60
CELA (298 K)							
Mean Value	30.93	16.63	25.07	309.2	39.52	36.81	31.41
ACBM-MCM	10.36	1.382	14.44	174.0	14.76	6.377	18.72
MCM-CBIV	4.091	1.442	14.76	202.8	47.74	4.732	11.32
ACBM-CBIV	11.93	0.0667	0.3192	32.55	32.97	2.692	9.376
CLAR (298 K)							
Mean Value	31.87	7.293	20.13	273.1	40.60	23.98	24.22
ACBM-MCM	9.892	1.187	10.90	156.0	15.96	5.290	15.60
MCM-CBIV	3.769	1.185	11.29	184.4	50.51	3.764	9.569
ACBM-CBIV	12.46	0.0672	0.4154	31.50	34.54	2.120	7.270
HAWT (298 K)							
Mean Value	16.22	3.884	11.03	174.4	15.84	13.68	10.61
ACBM-MCM	4.161	0.4206	4.720	71.92	7.476	1.481	3.987
MCM-CBIV	2.738	0.4410	4.947	85.62	19.78	1.714	1.720
ACBM-CBIV	4.346	0.0704	0.2424	15.69	12.31	0.9713	3.330
LBCC (298 K)							
Mean Value	28.87	16.28	26.72	287.7	24.33	36.79	24.51
ACBM-MCM	6.762	1.868	12.45	136.3	9.165	4.381	4.989
MCM-CBIV	2.247	1.913	12.606	158.0	28.21	5.034	2.807
ACBM-CBIV	7.885	0.0638	0.2901	25.26	19.05	2.761	7.418
RIVR (298 K)							
Mean Value	39.23	18.74	20.56	312.4	42.23	35.79	34.13
ACBM-MCM	10.08	2.520	15.16	175.5	15.72	6.579	15.88
MCM-CBIV	4.323	2.574	15.41	208.0	49.94	4.832	7.997
ACBM-CBIV	12.33	0.0589	0.2500	35.01	34.22	3.191	9.766
SNI (298 K)							
Mean Value	4.712	0.3838	1.089	59.79	5.040	0.9340	1.805
ACBM-MCM	0.7162	0.0741	0.5030	13.44	3.129	0.1410	0.8393
MCM-CBIV	1.699	0.0796	0.5400	18.923	7.495	0.1238	0.7765
ACBM-CBIV	1.411	0.0071	0.0401	5.485	4.366	1.1202	0.5083

[a]Note: Refer to Eq. (1) in the text for the method of calculating average values.

simulation and a 500-box simulation. Table 6 shows that vectorization techniques in SMVGEAR II reduced computer time by a factor of 4–7 per cell on the SGI Origin 2000 during multiple-cell calculations, in comparison with single-cell calculations, even though this machine is a scalar machine. The reduction on the Cray

Table 5
Spare-matrix reductions for the three mechanisms[a]

	Initial	After sparse matrix reductions			
		Day	% Reduction	Night	% Reduction
(a) CBIV					
Order of matrix	33	33	0	33	0
No. init. matrix spots filled	1089	292	73.19	283	74.01
No. fin. matrix spots filled	1089	323	70.34	315	71.07
No. operations decomp. 1	11,440	676	94.09	637	94.43
No. operations decomp. 2	528	166	68.56	159	69.89
No. operations backsub. 1	528	166	68.56	159	69.89
No. operations backsub. 2	528	124	76.52	123	76.70
(b) ACBM					
Order of matrix	109	109	0	109	0
No. init. matrix spots filled	11,881	822	93.08	797	93.29
No. fin. matrix spots filled	11,881	1008	91.52	982	91.73
No. operations decomp. 1	425,754	2150	99.50	2038	99.52
No. operations decomp. 2	5886	504	91.44	485	91.76
No. operations backsub. 1	5886	504	91.44	485	91.76
No. operations backsub. 2	5886	395	93.29	388	93.41
(c) MCM					
Order of matrix	1427	1427	0	1427	0
No. init. matrix spots filled	2,036,329	14,276	99.30	12,820	99.37
No. fin. matrix spots filled	2,036,329	17,130	99.16	14,947	99.27
No. operations decomp. 1	967,595,901	47,596	99.995	36,974	99.996
No. operations decomp. 2	1,017,451	9294	99.09	7393	99.27
No. operations backsub. 1	1,017,451	9294	99.09	7393	99.27
No. operations backsub. 2	1,017,451	6409	99.37	6127	99.40

[a]Note: Decomp. 1,2, and backsub. 1,2 refer to the first and second loops of matrix decomposition and backsubstitution, respectively.

Table 6
Computer time required per day of simulation for the three mechanisms

Case	CBIV	ACBM	MCM
(a) On an SGI origin 2000			
One cell (s day^{-1})	0.5360	3.088	36.87
500 cells (s day^{-1})	63.35	210.2	4949
Savings of vectorization	4.230	7.345	3.725
(b) on a Cray J90			
One cell (s day^{-1})	2.209	5.798	87.32
500 cells (s day^{-1})	29.45	75.15	1063
Savings of vectorization	37.50	38.58	41.07

J90 during multiple-cell calculations is more considerable (a factor of 40), since this machine is a vector machine. The reason is described in Jacobson (1998b). Based on the statistics provided here, it appears difficult, in terms of computer speed, to use Gear's original code to solve equations in the MCM mechanism, even in one box, without sparse-matrix reductions.

5. Conclusions

We compared the well-known carbon bond IV (CBIV) chemical mechanism (33 species, 81 reactions) with an adjusted carbon bond mechanism (ACBM) (109 species, 233 reactions) and a more explicit master chemical mechanism (MCM) (1427 species, 3911 reactions) in tests of their predictions of O_3, NO_x (= NO + NO_2), HCHO, HNO_3, H_2O_2, and peroxyacetlynitrate (PAN). All three mechanisms tested were updated with the inorganic chemistry from the ACBM and implemented into the sparse-matrix, ordinary differential equation solver, SMVGEAR II. We found that sparse-matrix treatment in SMVGEAR II reduced the number of calculations during matrix decomposition for the MCM by a factor of 15,000 (99.995%), or from an estimated 154 h to 37 s of cpu time per simulation day in one cell on an SGI Origin 2000, in comparison with a full-matrix solution. Computer time for each mechanism was linearly proportional to the number of species in the mechanism. It is shown that the three mechanisms agreed closely when aromatic concentrations were initially low in comparison with alkane, alkene, and aldehyde initial concentrations.

When aromatic concentrations were initially high (higher than that observed in urban air), the yields of O_3, HCHO, and PAN differed significantly among the three mechanisms although the daily maximum concentrations of these species agreed better. The aromatic representation in MCM leads to systematic overprediction of ozone, according to comparisons with smog chamber data. For initial conditions taken from measurements at nine sites in Los Angeles, the daily maximum concentrations of O_3, HCHO, PAN and H_2O_2 predicted by the three mechanisms differed by 30–50%, 10–40%, 15–40%, and 60–80%, respectively. The relative differences between the daytime time series of O_3, HCHO, H_2O_2, and PAN predicted by the three mechanisms were 7–68%, 7–46%, 35–150%, and 10–64%, respectively, The replacement of the aromatic scheme of MCM with that of ACBM significantly reduced the disagreement with respect to ozone. Since the atmospheric reactivity of many intermediate species in MCM is poorly understood, the uncertainties in the hypothetical chemical reactions of these species and the hypothetical reaction rate constants may be responsible for the large difference. The measurement of H_2O_2 in smog chamber experiments would be useful in validating chemical mechanisms.

References

Andersson-Skold, Y., Simpson, D., 1999. Comparison of the chemical scheme of the EMEP MSC-W and IVL photochemical trajectory models. Atmospheric Environment 33, 1111–1129.

Atkinson, R., Lloyd, A.C., Winges, L., 1982. An updated chemical mechanism for hydrocarbon/NO_x/SO_2 photooxidations suitable for inclusion in atmospheric simulation models. Atmospheric Environment 16, 1341–1355.

Atkinson, R.A., Baulch, D.L., Cox, R.A., Hampson Jr., R.F., Kerr, J.A., Rossi, M.J., Troe, J., 1997. Evaluated kinetic, photochemical, and heterogeneous data for atmospheric chemistry: supplement V IUPAC subcommittee on gas kinetic data evaluation for atmospheric chemistry. Journal of Physical Chemistry Reference Data 26, 521–1011.

Carter, W.P.L., 1990. A detailed mechanisms for the gas-phase atmospheric reactions of organic compounds. Atmospheric Environment 24A, 481–518.

Chock, D.P., Yarwood, G., Dunker, A.M., Morris, R.E., Pollack, A.K., Schleyer, C.H., 1995. Sensitivity of urban airshed model results for test fuels to uncertainties in light-duty vehicle and biogenic emissions and alternative chemical mechanisms: auto oil air-quality improvement research program. Atmospheric Environment 29, 3067–3084.

DeMore, W.B., Sanders, S.P., Golden, D.M., Hampson, R.F., Kurylo, M.J., Howard, C.J., Ravishankara, A.R., Kolb, C.E., Molina, M.J., 1997. Chemical kinetics and photochemical data for use in stratospheric modeling. Evaluation number, Vol. 12. JPL Publ. 97-4, Jet Propulsion Laboratory, Pasadena, CA.

Dodge, M.C., 1989. A comparison of three photochemical oxidant mechanisms. Journal of Geophysical Research 94, 5121–5136.

Gery, M.W., Witten, G.Z., Killus, J.P., 1988. Development and testing of the CBM-IV for urban and regional modeling. Rep. EPA-600/3-88-012, U.S. EPA. Research Triangle Park, North Carolina.

Gery, M.W., Whitten, G.Z., Killus, J.P., Dodge, M.C., 1989. A photochemical kinetics mechanism for urban and regional scale computer modeling. Journal of Geophysical Research 94, 12925–12956.

Hertel, O., Christensen, J., Runge, E.H., Asman, W.A.H., Berkowicz, R., Hovmand, M.F., Hov, O., 1995. Development and testing of a new variable scale air-pollution model: ACDEP. Atmospheric Environment 29, 1267–1290.

Houweling, S., Dentener, F., Lelieveld, J., 1998. The impact of nonmethane hydrocarbon compounds on tropospheric photochemistry. Journal of Geophysical Research 103, 10673–10696.

Jacobson, M.Z., 1995. Computation of global photochemistry with SMVGEAR II. Atmospheric Environment 29, 2541–2546.

Jacobson, M.Z., 1997. Development and application of a new air pollution modeling system. Part III: aerosol-phase simulations. Atmospheric Environment 31A, 587–608.

Jacobson, M.Z., 1998a. Studying the effects of aerosols on vertical photolysis rate coefficient and temperature profiles over an urban airshed. Journal of Geophysical Research 103, 10593–10604.

Jacobson, M.Z., 1998b. Improvement of SMVGEAR II on vector and scalar machines through absolute error tolerance control. Atmospheric Environment 32, 791–796.

Jacobson, M.Z., 1999a. Fundamentals of Atmospheric Modeling. Cambridge Univ. Press, New York.

Jacobson, M.Z., 1999b. Isolating nitrated and aromatic aerosols and nitrated aromatic gases as sources of ultraviolet light absorption. Journal of Geophysical Research 104, 3527–3542.

Jacobson, M.Z., 1999c. Studying the effects of soil moisture on ozone, temperatures, and winds in Los Angeles. Journal of Applied Meteorology 38, 607–616.

Jacobson, M.Z., Turco, R.P., 1994. SMVGEAR: a sparse-matrix, vectorized Gear code for atmospheric models. Atmospheric Environment 28 (A), 273–284.

Jacobson, M.Z., Lu, R., Turco, R.P., Toon, O.B., 1996. Development and application of a new air pollution modeling system. Part I: Gas-phase simulations. Atmospheric Environment 30B, 1939–1963.

Jeffries, H.E., Sexton, K.G., Arnold, J.R., Li, J.L., 1988. Validation testing of new mechanisms with outdoor chamber data, Vol. 1, Comparison of CB4 and CAL Mechanisms. EPA Cooperative Agreement 813107. U.S. Environmental Protection Agency, Research Triangle Park, NC.

Jenkin, M.E., Saunders, S.M., Pilling, M.J., 1997. The tropospheric degradation of volatile organic compounds: a protocol for mechanism development. Atmospheric Environment 31, 81–104.

Kasibhatla, P., Chameides, W.L., Duncan, B., Houyoux, M., Jang, C., Mathur, R., Odman, T., Xiu, A., 1997. Impact of inert organic nitrate formation on ground-level ozone in a regional air-quality model using the carbon bond mechanism 4. Geophysical Research Letters 24, 3205–3208.

Lurmann, F.W., Carter, W.P.L., Coyner, L.A., 1987. A surrogate species chemical reaction mechanism for urban scale air quality simulation models, Vol. I, Adaption of the mechanism. EPA-600/3-87/014a, U.S. Environmental Protection Agency, Research Triangle Park, NC.

Madronich, S., Calvert, J.G., 1990. Permutation reactions of organic peroxy radicals in the troposphere. Journal of Geophysical Research 95, 5697–5715.

Stockwell, W.R., 1986. A homogeneous gas-phase mechanism for use in a regional acid deposition model. Atmospheric Environment 20, 1615–1632.

Stockwell, W.R., Middleton, P., Chang, J.S., Tang, X., 1990. The second generation regional acid deposition model chemical mechanism for regional air quality modeling. Journal of Geophysical Research 95, 16343–16367.

Stockwell, W.R., Kirchner, F., Kuhn, M., Seefeld, S., 1997. A new mechanism for regional atmospheric chemistry modeling. Journal of Geophysical Research 102, 25847–25879.

Whitten, G.Z., Hogo, H., Killus, J.P., 1980. The carbon bond mechanism: a condensed kinetic mechanism for photochemical smog. Environmental Science and Technology 14, 690–700.